View metadata, citation and similar papers at core.ac.uk

brought to you by CORE

provided by MURAL - Maynooth University Research Archive Library

The Journal of Chemical Physics

Spectroscopic characterization of the weakly bound $Ca(4s4d\sigma\ ^3D_3)\cdot Ar[^3\Sigma^+]$ state: Evidence for a substantial maximum in the potential curve at long range

Cite as: J. Chem. Phys. **111**, 2484 (1999); https://doi.org/10.1063/1.479526
Submitted: 13 April 1999 . Accepted: 13 May 1999 . Published Online: 28 July 1999

Allen W. K. Leung, John G. Kaup, D. Bellert, John G. McCaffrey, and W. H. Breckenridge

View Online Export Citation

ARTICLES YOU MAY BE INTERESTED IN

Two-electron pseudopotential investigation of the electronic structure of the CaAr molecule
The Journal of Chemical Physics **117**, 7534 (2002); https://doi.org/10.1063/1.1506921

Spectroscopic characterization of the metastable $4p\pi\ ^2\Pi_{0^-}$ valence states and the $5s\ ^3\Sigma^+$ Rydberg states of the CaAr, CaKr, and CaXe van der Waals molecules
The Journal of Chemical Physics **107**, 5283 (1997); https://doi.org/10.1063/1.474238

Resonant two-color photoionization threshold measurements of the $Zn^+(4s)\cdot Ar$ bond strength: Model-potential analysis of $M^+(ns)\cdot Ar$ interactions
The Journal of Chemical Physics **110**, 6298 (1999); https://doi.org/10.1063/1.478534

Lock-in Amplifiers
Find out more today

Zurich Instruments

© 1999 American Institute of Physics.

Spectroscopic characterization of the weakly bound Ca($4s4d\sigma\ ^3D_3$) $\cdot$Ar[$^3\Sigma^+$] state: Evidence for a substantial maximum in the potential curve at long range

Allen W. K. Leung, John G. Kaup,[a] D. Bellert, John G. McCaffrey,[b] and W. H. Breckenridge
Department of Chemistry, University of Utah, Salt Lake City, Utah 84112

(Received 13 April 1999; accepted 13 May 1999)

The weakly bound Ca($4s4d\sigma\ ^3D_3$)$\cdot$Ar[$^3\Sigma^+$] state has been characterized by means of R2PI (Resonant Two-Photon Ionization) spectroscopy, using transitions from the Ca($4s4p\pi\ ^3P_0$) $\cdot$Ar[$^3\Pi_{0^-}$] metastable state prepared in a laser-vaporization/supersonic jet source. Because several of the vibrational levels are above the dissociation limit [to Ca($4s4d\ ^3D_3$)+Ar($^1S_0$)], it is concluded that there must be a substantial maximum in the Ca($4s4d\sigma\ ^3D_3$)$\cdot$Ar[$^3\Sigma^+$] potential curve (>200 cm^{-1}) at large R (>4.0 Å). This is discussed, and shown to be consistent with our earlier ideas of ''penetration'' of outerlobes of electron density of metal atom excited states by RG (rare-gas) atoms. Perturbations observed, due to possible potential curve crossings with states of different electronic symmetry, are also discussed. © *1999 American Institute of Physics.*
[S0021-9606(99)00730-8]

INTRODUCTION

Duval *et al.* experimentally characterized[1] the first case of a long-range potential curve maximum in a M*$\cdot$RG excited state (M*=electronically excited metal atom, RG=rare-gas atom) which was not due to an adiabatic avoided potential-curve crossing, when they showed, by means of careful laser double-resonance experiments, that the Hg($6s7s\ ^3S_1$)$\cdot$Ar[$^3\Sigma^+$] excited Rydberg state had a small (~15 cm^{-1}) maximum in its potential curve at large R (~5 Å). They argued[1] that the maximum was at much too large a value of R to result from a curve crossing with the only other lower-lying HgAr($^3\Sigma^+$) state, and postulated that the maximum was due to exchange repulsion of the Ar atom electrons with the outerlobe electron density of the Hg($7s$) Rydberg electron.[1,2] At shorter internuclear distances R, Breckenridge *et al.* postulated[1,2] that the Ar atom had substantially ''penetrated'' the diffuse Hg($7s$) electron cloud, and thus experienced strong attractive forces somewhat akin to those in the Hg$^+$($6s$)$\cdot$Ar free ion [which has R_e,D_e values very similar to those of the Hg($6s7s\ ^3S_1$)$\cdot$Ar[$^3\Sigma^+$] Rydberg state]. Since then, several examples of these kinds of potential-curve maxima have either been demonstrated directly, or inferred, by our group as well as by others.[3–13] Theoretical *ab initio* calculations have also shown[10,14–16] such maxima, in cases where avoided curve crossings are quite unlikely, confirming the original ''penetration'' hypothesis[1,2] of Breckenridge *et al.* for such Rydberg states.

For M*($np\sigma$)$\cdot$RG or M*($nd\sigma$)$\cdot$RG excited states, the M* outer electron density is more concentrated along the bond axis as the RG atom approaches than for M*(ns)$\cdot$RG states, where the M*(ns) electron density is uniformly distributed (angularly), so that larger potential maxima might well be expected. We report here an experimental spectroscopic characterization of the excited Ca($4s4d\sigma\ ^3D_3$)$\cdot$Ar[$^3\Sigma^+$] state (formally ''valence'' in character) which shows that there must be a long-range maximum in the potential curve of at least 200 cm^{-1} at R>4.0 Å, and that the actual bond strength (D_0) is only 134±50 cm^{-1}. The bonding, as well as small perturbations apparently due to potential-curve crossings of states of other electronic symmetries, is discussed.

II. EXPERIMENT

These experiments were carried out using an apparatus constructed for the spectroscopy of, and dynamics within, atom-(RG)$_n$, and atom-(molecule)$_n$ van der Waals complexes using either laser-induced fluorescence (LIF) or resonance two-photon ionization (R2PI) detection. The apparatus is described in more detail elsewhere.[17–19]

Briefly, calcium vapor was produced by focusing the second harmonic of a Molectron MY-32/10 Q-switched Nd:YAG laser onto a calcium target rod (1/4 in. diam machined from Alpha/Aesar 99% pure ingot). An 800 μs pulse of gas produced by a double-solenoid pulsed valve operated at 40 psi Ar backing pressure passed over the calcium rod coincident with the vaporization laser pulse. The Ca vapor/argon pulse then passed through a 1.8 mm orifice after having traveled 4 mm from the site of vaporization into the chamber maintained at 6×10^{-4} Torr. The beam, after passing through a 5 mm diam skimmer 20 cm from the source, entered the ionization region of a time-of-flight mass spectrometer at a total distance of 60 cm from the source. R2PI spectra are obtained by scanning the output of a dye laser to

[a]Present address: Department of Chemistry, Furman University, Greenville, SC 29613.
[b]Visiting Associate Professor, University of Utah, 1998. Permanent address: Department of Chemistry, National University of Ireland, Maynooth, Co. Kildare, Ireland.

 © 1999 American Institute of Physics

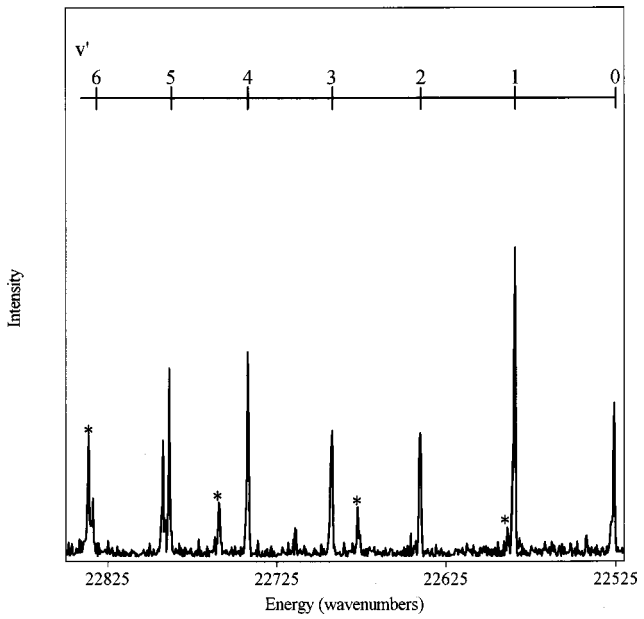

FIG. 1. Low resolution spectrum of the $Ca(4s4d\sigma\,^3D_3)\cdot Ar[^3\Sigma^+]$, $v' \leftarrow Ca(4s4p\pi\,^3P_0)\cdot Ar[^3\Pi_{0^-}]$, $v''=0$ vibrational progression. [Transitions to the $Ca(4p\pi4p\pi\,^3P_J)\cdot Ar[^3\Sigma^-]$ state are indicated by asterisks.]

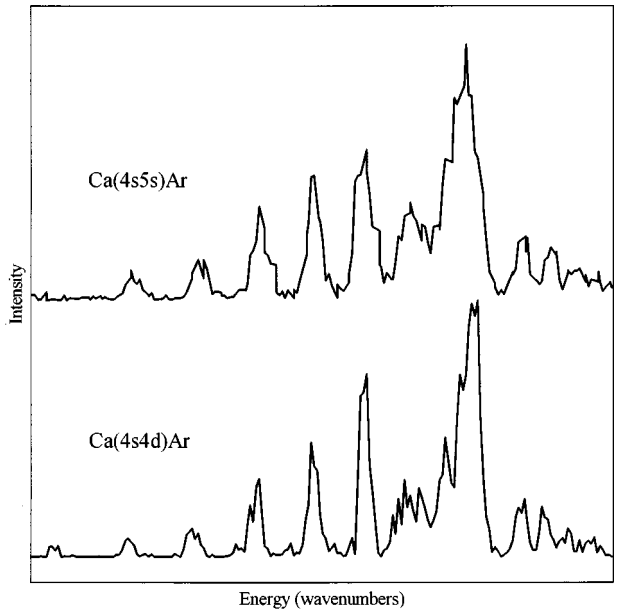

FIG. 2. (a) High-resolution spectrum of the (5,0) band of the transition to the $Ca(4s5s\,^3S_1)\cdot Ar[^3\Sigma^+]$ state. (b) High-resolution spectrum of the band at 22 639.7 cm^{-1} in Fig. 1. (The horizontal axis scale for the two spectra, in cm^{-1}, is the same.)

excite transitions from the $Ca(4s4p\pi\,^3P_J)\cdot RG(^3\Pi_{0^-}, v''=0, J'')$ metastable states. Photoionization with a simultaneously pumped ionization dye laser created ions which were detected after a 1 m free-flight region. Dyes used: Coumarin 480 (resonance), Coumarin 500(ionization).

III. RESULTS AND DISCUSSION

A. Assignment of the electronic symmetry and the asymptotic atomic states of the upper state

We recently reported[20] the spectroscopic characterization of the $Ca(4s4d\pi\,^3D_J)\cdot Ar[^3\Pi_{0^-}]$, $Ca(4s4d\delta\,^3D_1)\cdot Ar[^3\Delta_1]$ states, and the unusually strongly bound doubly excited $Ca(4p\pi4p\pi\,^3P_J)\cdot Ar[^3\Sigma^-]$ state, by laser excitation of the $Ca(4s4p\pi\,^3P_0)\cdot Ar[^3\Pi_{0^-}]$ metastable state in the 22 000–23 300 cm^{-1} energy region. We now report the spectroscopic characterization of several bands of another vibrational progression in the 22 500–22 900 cm^{-1} region (see Fig. 1) which originally puzzled us. The rotational structure of some of the bands is virtually identical to bands in the 15 800–16 400 cm^{-1} region which we earlier successfully simulated[13] as $Ca(4s5s\,^3S_1)\cdot Ar[^3\Sigma^+]\leftarrow Ca(4s4p\pi\,^3P_0)\cdot Ar[^3\Pi_{0^-}]$ transitions. [The upper state in this case *must* be of $^3\Sigma^+$ symmetry, since the $Ca(4s5s\,^3S_1)$ state is the only asymptotic triplet atomic state of Ca within 4000 cm^{-1}.[13]] For example, shown in Fig. 2(a) is a high-resolution spectrum of the (5,0) band of the $5s\,^3\Sigma^+$ transition[13] as compared to [Fig. 2(b)] a high-resolution spectrum of the band at 22 639.7 cm^{-1} in the progression of Fig. 1.

Shown in Fig. 3 are the rotational branches expected for a $^3\Sigma^+(b)\leftarrow{}^3\Pi_{0^+,0^-}$-(a) transition. Since only the lowest energy multiplet, $Ca(4s4p\pi\,^3P_0)\cdot Ar[^3\Pi_{0^-}]$, is known to be populated under our conditions,[13] there is one *S*-type branch spread out to the blue, three degenerate *Q*-type branches spread slightly to the blue of the band origin, and an *O*-type branch which heads to the red. All of the five bands in the progression in Fig. 1 which we have been able to simulate successfully have this same kind of structure, so we can clearly assign the electronic symmetry of the upper state in

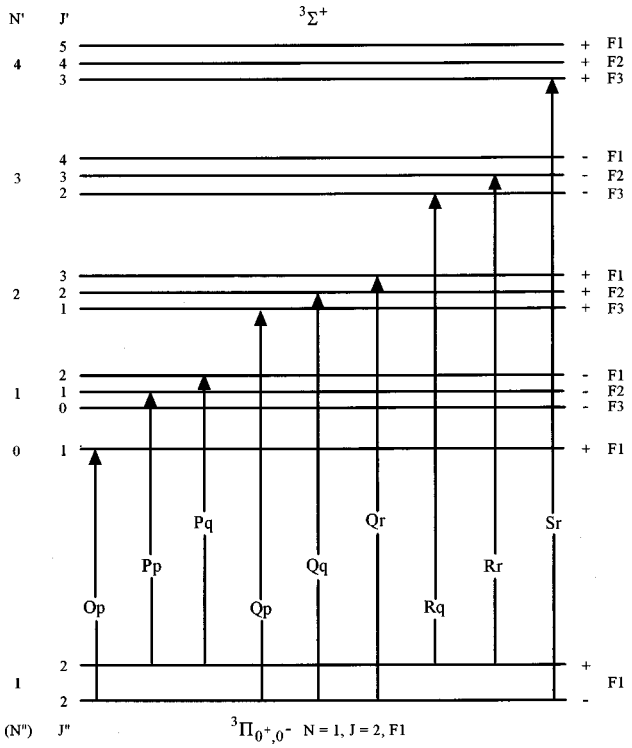

FIG. 3. Schematic diagram showing the rotational branches for $^3\Sigma^+$ (case ''b'') $\leftarrow{}^3\Pi_{0^+,0^-}$ (case ''a'') transitions. Branch notation: Capitol letter indicates the ''form'' of the branch, $N'\leftarrow J''$, while the small letter following indicates the $J'\leftarrow J''$ character of the branch. For example, for an Sr branch $N'=J''+2$, and $J'=J''+1$.

the progression in Fig. 1 as $^3\Sigma^+$. (But see below for further discussion of two of these bands.) One of the problems with this assignment, however, is that a linear Birge–Sponer extrapolation of the bands yields an approximate dissociation limit [given the estimated $D_0 = 60 \pm 50\ \mathrm{cm}^{-1}$ of the $\mathrm{Ca}(4s4p\pi\ ^3P_0)\cdot\mathrm{Ar}[^3\Pi_{0^-}]$ lower state][20] which is nowhere near any asymptotic excited Ca* state which can yield a $\mathrm{CaAr}[^3\Sigma^+]$ molecular state.

The Birge–Sponer extrapolated dissociation limit is $38\,229\ \mathrm{cm}^{-1}$ [with $E=0$ set as $\mathrm{Ca}(4s^2\ ^1S_0)+\mathrm{Ar}$]. The closest asymptotic states,[21] $\mathrm{Ca}(3d4p\ ^3D_J^0)$ at 38 192–38 259 cm^{-1}, can only produce $^3\Sigma^-$, $^3\Pi$, and $^3\Delta$ states when bound to Ar.[22] The $\mathrm{Ca}(4p^2\ ^3P_J)$ states, at 38 418–38 551 cm^{-1}, can also only yield $^3\Sigma^-$ and $^3\Pi$ states when bound to Ar.[22] The next highest states, $\mathrm{Ca}(3d4p\ ^3P_J^0)$ at 39 333–39 340 cm^{-1}, can yield $^3\Sigma^+$ and $^3\Pi$ states,[22] but this would require a huge bond energy for the observed $^3\Sigma^+$ state of $D_0 \approx 1709\ \mathrm{cm}^{-1}$. Not only is this very unlikely, since the wave function of this $^3\Sigma^+$ state must have *some* $3d\sigma 4p\sigma$ character which will be *extremely* repulsive in nature (in addition, of course, to attractive $3d\pi_{+1}4p\pi_{-1}$ character) it would also require that the true dissociation energy be more than 1100 cm^{-1} greater than the extrapolated linear Birge–Sponer value of ~605 cm^{-1}. Although true dissociation energies of these kinds of complexes are often slightly greater than the linear Birge–Sponer values due to the fact that a Morse potential function cannot correctly represent the dispersive attractive forces near dissociation, this is far outside such expected minor differences, and $\mathrm{Ca}(3d4p\ ^3P_J^0)+\mathrm{Ar}$ therefore cannot be the dissociation limit for this $^3\Sigma^+$ state. The R_0 value (3.31 Å) is also much too large for a state bound by ~1700 cm^{-1}; the very strongly bound ''pure-π'' $\mathrm{Ca}(4p\pi 4p\pi\ ^3P_J)\cdot\mathrm{Ar}[^3\Sigma^-]$ state ($D_0 = 1278\ \mathrm{cm}^{-1}$) has an R_0 value of <3.0 Å (see below, and Fig. 8). Finally, the vibrational frequency, ~61 cm^{-1}, is about half that of the strongly bound $\mathrm{Ca}(4p\pi 4p\pi\ ^3P_J)\cdot\mathrm{Ar}[^3\Sigma^-]$ state,[20] ~118 cm^{-1}.

We are therefore forced to conclude that the only reasonable dissociation limit for this state is the lower-lying $\mathrm{Ca}(4s4d\ ^3D_3)$ state, which yields a $^3\Sigma^+$ state with $\mathrm{Ca}(4d\sigma)$ alignment with respect to the Ar atom. Because several of the observed vibrational levels are *above* the asymptotic energy of $\mathrm{Ca}(4s4d\ ^3D_3)+\mathrm{Ar}$, the potential curve of the $\mathrm{Ca}(4s4d\sigma\ ^3D_3)\cdot\mathrm{Ar}[^3\Sigma^+]$ state must have a substantial *maximum* (>200 cm^{-1}) at large internuclear distances (R >4.0 Å). This is actually quite a reasonable possibility, as we discuss below.

B. Vibrational assignments

The moderately strong band at 22 525.7 cm^{-1} in Fig. 1 was assigned as the (0,0) band, since there was absolutely no sign of another band to the red at the energy expected from the band origin progression. (The signal-to-noise was too low for reliable $^{40}\mathrm{Ca}^{40}\mathrm{Ar}/^{44}\mathrm{Ca}^{40}\mathrm{Ar}$ isotopic splitting measurements, since ^{44}Ca has an isotopic abundance of only 2.1%; Ar is essentially monoisotopic.)

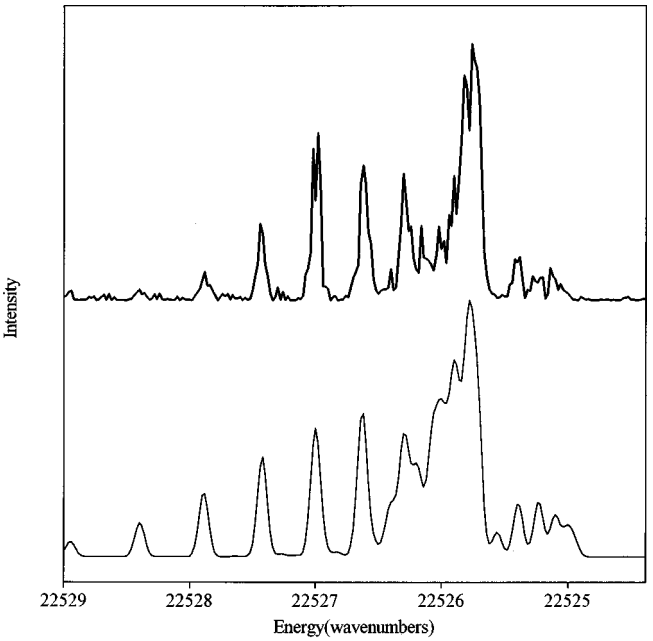

FIG. 4. High-resolution spectrum of the (0,0) band. Computer simulation is shown below. Simulation parameters: $B_0'' = 0.0555\ \mathrm{cm}^{-1}$, $B_0' = 0.0761\ \mathrm{cm}^{-1}$, $T = 0.8°$ K, laser linewidth: 0.09 cm^{-1}, $\lambda_{\mathrm{S.S.}} = -0.12\ \mathrm{cm}^{-1}$ (see text).

C. Rotational analysis

Shown in Figs. 4–8 are high-resolution spectra of the $(v',0)$ bands ($v' = 0-4$), along with the successful computer simulations of the band contours, assuming a $^3\Sigma^+(b) \leftarrow {}^3\Pi_0\text{-}(a)$ transition, as discussed above. For the (1,0), (2,0), and (3,0) bands, the spin–spin splitting constant was successfully set to zero [as was the case with all the $\mathrm{Ca}(4s5s\ ^3S_1)\cdot\mathrm{Ar}[^3\Sigma^+] \leftarrow \mathrm{Ca}(4s4p\pi\ ^3P_0)\cdot\mathrm{Ar}[^3\Pi_{0^-}]$ transitions simulated earlier].[13] For the (0,0) and (4,0) bands, however, small spin–spin splitting constants of $\lambda_{\mathrm{S.S.}} \approx -0.12\ \mathrm{cm}^{-1}$ were absolutely required to get a reasonable

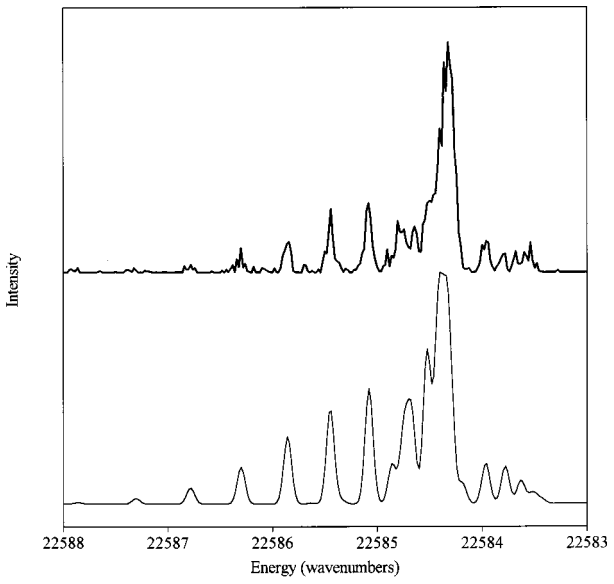

FIG. 5. Same as Fig. 4, but (1,0) band. $B_1' = 0.0741\ \mathrm{cm}^{-1}$, $\lambda_{\mathrm{S.S.}} = 0.00\ \mathrm{cm}^{-1}$.

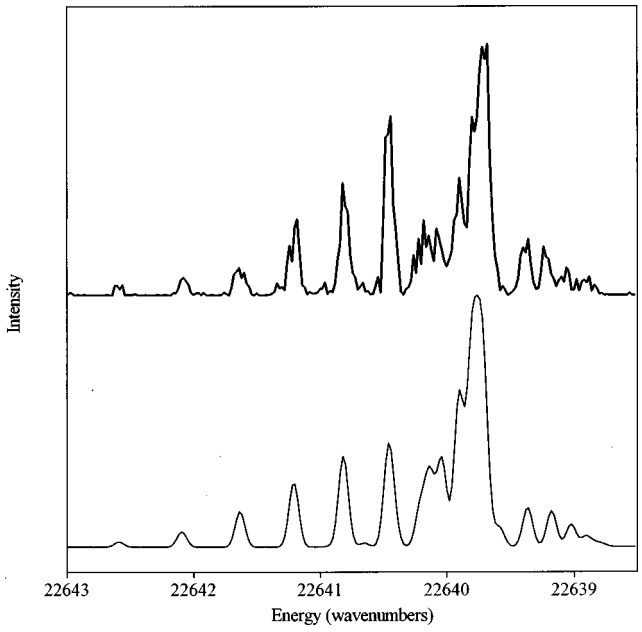

FIG. 6. Same as Fig. 4, but (2,0) band. $B_2'=0.0721\ \mathrm{cm}^{-1}$, $\lambda_{S.S.}=0.00\ \mathrm{cm}^{-1}$.

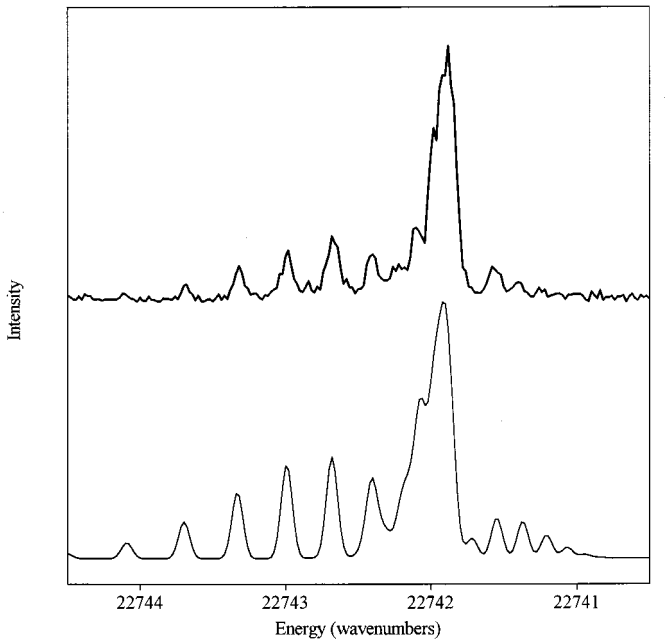

FIG. 8. Same as Fig. 4, but (4,0) band. $B_4'=0.0679\ \mathrm{cm}^{-1}$, $\lambda_{S.S.}=-0.11\ \mathrm{cm}^{-1}$.

fit. ''Spin–spin'' splitting[23,24] causes the degenerate J levels of each N level to split, until at high values of $\lambda_{S.S.}$ the $^3\Sigma^+(b)$ state evolves into two case ''c'' type states ($\Omega=0^-$ and $\Omega=\pm1$).[23] (For a heavy atom like Ca, true ''spin–spin'' coupling is very small, and the ''spin–spin'' splitting is actually due to second-order spin-orbit coupling.[24])

The signal-to-noise of the (6,0) band was too low for rotational analysis, and we have also been unable to simulate satisfactorily the rotational structure of the (5,0) band assuming a simple $^3\Sigma^+(b)\leftarrow{}^3\Pi_0-(a)$ transition and either positive or negative $\lambda_{S.S.}$ values up to several cm^{-1}. There is also an ''extra'' unassigned band $\sim3.5\ \mathrm{cm}^{-1}$ to the blue of the (5,0) band, which could also not be simulated satisfactorily. The (5,0) band thus appears to be severely perturbed, and we will discuss possible perturbing states later. The band origins, and B_v' values for the fit bands, are listed in Table I. The spectroscopic constants for the upper and lower states are listed in Table II.[25] The small D_o (and D_e) values listed in Table II for the $\mathrm{Ca}(4s4d\sigma\,{}^3D_3)\cdot\mathrm{Ar}[{}^3\Sigma^+]$ state are calculated via a thermochemical cycle:

$$D_o(^3\Sigma^+)=D_o(^3\Pi_{0^-})+E(^3D_3)-E(^3P_0)-\nu_{0,0}$$

using an estimate[20] of $D_0(^3\Pi_{0^-})=60\pm50\ \mathrm{cm}^{-1}$.

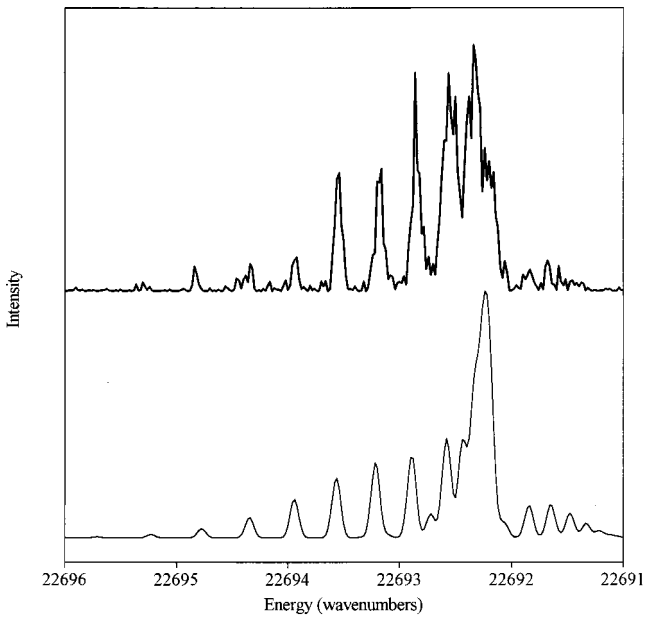

FIG. 7. Same as Fig. 4, but (3,0) band. $B_3'=0.0698\ \mathrm{cm}^{-1}$, $\lambda_{S.S.}=0.00\ \mathrm{cm}^{-1}$.

D. Possible perturbations of the $\mathrm{Ca}(4s4d\sigma\,{}^3D_3)\cdot\mathrm{Ar}[{}^3\Sigma^+]$ levels by curve crossings

Shown in Fig. 9 are our estimates of the potential curves of the states in this energy region which have been characterized spectroscopically. The unusual, strongly bound $\mathrm{Ca}(4p\pi4p\pi\,{}^3P_J)\cdot\mathrm{Ar}[{}^3\Sigma^-]$ state is severely predissociated,[20] washing out all rotational structure, but D_e is accurately known. We estimated the R_e value for this $^3\Sigma^-$ state by Franck–Condon simulations of the low-resolution

TABLE I. Band origins and $B_{v'}$ values for the $\mathrm{Ca}(4s4d\sigma\,{}^3D_3)\cdot\mathrm{Ar}[{}^3\Sigma^+]-\mathrm{Ca}(4s4p\pi\,{}^3P_0)\cdot\mathrm{Ar}[{}^3\Pi_{0^-}]$ transitions ($B_0''=0.0555\ \mathrm{cm}^{-1}$). Values for (5,0) and (6,0) bands are from low-resolution spectra.

Band	Band origin (cm^{-1})	$B_{v'}$ (cm^{-1})
(0,0)	22 525.7	0.0761
(1,0)	22 584.3	0.0741
(2,0)	22 639.7	0.0721
(3,0)	22 692.1	0.0698
(4,0)	22 741.8	0.0679
(5,0)	22 788.8	-
(6,0)	22 833.8	-

TABLE II. Spectroscopic constants of the $Ca(4s4p\pi\,^3P_0)\cdot Ar[^3\Pi_{0^-}]$ and $Ca(4s4d\sigma\,^3D_3)\cdot Ar[^3\Sigma^+]$ states. All units in cm^{-1}, except R_e and R_o, which are in Å.

	$^3\Pi_{0^-}$	$^3\Sigma^+$
$\nu_{0,0}$	.....	22 525.7
ω_e	.....	61.48±0.43
$\omega_e x_e$	.....	1.49±0.079
B_o	0.0555±0.003 00[a,b]	0.0782±0.0030
B_e	.....	0.0772±0.0030
α_e	.....	0.002 07±0.000 10
R_o	3.90±0.10[a,b]	3.31±0.06
R_e	.....	3.29±0.06
D_o	60±50[c]	134±50
D_e	.....	164±50

[a]Reference 20.
[b]Reference 13.
[c]Reference 25.

vibrational progression,[20] knowing $R_o=3.90$ Å for the $Ca(4s4p\pi\,^3P_0)\cdot Ar[^3\Pi_{0^-}]$ lower state.[13] Also shown in this figure are the $v'=0-6$ vibrational levels of the $^3\Sigma^+$ state. Note that the $^3\Sigma^-$ potential curve crosses the $^3\Sigma^+$ potential curve near the $^3\Sigma^+(v'=0)$ vibrational level.

The ''$\Omega=0^+$'' levels of a $^3\Sigma^-$ state cannot interact with the ''$\Omega=0^-$'' levels of a $^3\Sigma^+$ state because they have opposite parities (*e* versus *f*, respectively). However, the *e*/*f* pairs of $\Omega=1$ levels of a $^3\Sigma^-$ state *can* interact with the *e*/*f* $\Omega=1$ pairs of levels of a $^3\Sigma^+$ state.[26] If the $^3\Sigma^-/^3\Sigma^+$ curve crossing is just above the $v'=0$ level of the $^3\Sigma^+$ state, as indicated, this would push the $\Omega=1$ level of the $^3\Sigma^+(v'=0)$ state *below* that of the $\Omega=0^-$ level, resulting in apparently *negative* values of $\lambda_{S.S.}$ for the $v'=0$ level, as observed. The interaction would be weak (as observed) since the $Ca(4p\pi_{+1}4p\pi_{-1})\cdot Ar[^3\Sigma^-]$ molecular orbital configuration is quite different from the $Ca(4s\sigma_0 4d\sigma_0)\cdot Ar[^3\Sigma^+]$ configuration, so that the coupling is probably determined by how ''mixed'' these states are with other configurations.

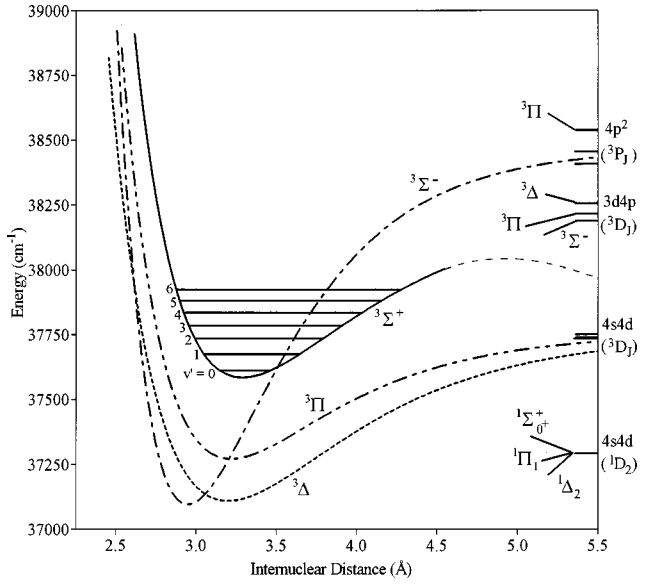

FIG. 9. Plots of the potential curves of the relevant CaAr excited states which have been characterized experimentally. (See text.)

(Because of the similar energies of the 3*d*, 4*s*, and 4*p* orbitals in Ca, there are several low-lying doubly excited atomic states,[21] and thus many possibilities.)

However, the $^3\Sigma^+/^3\Sigma^-$ crossing indicated in Fig. 9 cannot explain either the $\lambda_{S.S.}\approx -0.12\,cm^{-1}$ value for the $v'=4$ band nor the apparently strong perturbation of the $v'=5$ band. There will be another, fairly strongly bound $^3\Sigma^-$ state from the $Ca(3d4p\,^3D_1)+Ar$ asymptote, however (see Fig. 9): the ''pure-π'' $Ca(3d\pi_{+1}4p\pi_{-1}\,^3P_0)\cdot Ar[^3\Sigma^-]$ state. Now, if this state is slightly *less* bound than the ''pure-π'' $Ca(4p\pi 4p\pi\,^3P_J)\cdot Ar[^3\Sigma^-]$ state [there should be more repulsion with the Ar atom for $Ca(3d\pi)$ than for $Ca(4p\pi)$], the potential curve for this state might cross that for the $^3\Sigma^+$ state (shown in Fig. 9) *very* near the $v'=5$ level on the outer wing of the $^3\Sigma^+$ potential curve. If so, this could possibly account for the severe perturbation of the $v'=5$ level as well as the negative $\lambda_{S.S.}$ value for the $v'=4$ level as well, if the interaction is stronger than for the $v'=0$ perturbation. We admit this is quite speculative, but it is at least plausible.

There are also several other possibilities of curve-crossing couplings from states which evolve from *lower-energy* Ca*+Ar asymptotes:

1. $Ca(4s4d\,^1D_2)$ ($E=37\,298\,cm^{-1}$)

Oddly, this singlet atomic state is actually slightly lower in energy than the triplet $Ca(4s4d\,^3D_J)$ states because of mixing of higher-energy $Ca(4p4p\,^1D_2)$ character into the nominally $Ca(4s4d\,^1D_2)$ state, pushing it down in energy.[21] The molecular states possible are $^1\Sigma^+_{0^+}$, $^1\Pi_1$, and $^1\Delta_2$. The $^1\Pi$ state could interact specifically with the $^3\Sigma^+_1$ components, but this state should be fairly strongly bound (with a potential curve similar to that of the $4s4d\,^3\Pi$ state shown in Fig. 9), and thus should not cross the $4s4d\,^3\Sigma^+$ potential curve. The $^1\Sigma^+_{0^+}$ state (*e* parity) cannot interact directly with the $^3\Sigma^+_{0^-}$ state (*f* parity), and the $^1\Delta_2$ state $\Omega=2$ cannot interact with either of the $\Omega=0^-$,1 components of the $^3\Sigma^+$ state.

2. $Ca(4s5p\,^1P^0_1)$ and $Ca(4s5p\,^3P^0_J)$ ($E=36\,548-36\,732\,cm^{-1}$)

The $^1\Sigma^+$, $^1\Pi$, $^3\Sigma^+$, $^3\Pi$ Rydberg type states from these asymptotes are probably all too bound to cross the $^3\Sigma^+$ potential curve, and only the very bound $^1\Pi_1$ state could interact appropriately in any case.

3. $Ca(3d4p\,^1D^0_2)$ ($E=35\,835\,cm^{-1}$)

Of the $^1\Sigma^-$, $^1\Pi_1$, and $^1\Delta_2$ states possible here, the $^1\Sigma^-_{0^-}$ state could interact specifically with the $^3\Sigma^+_{0^-}$ component, and the $^1\Pi_1$ state could interact specifically with the $^3\Sigma^+_1$ components. However, the $^1\Sigma^-$ state will have a unique $3d\pi_{+1}4p\pi_{-1}$ type M.O. configuration, will thus be quite bound, and should not cross the higher-lying $4s4d\,^3\Sigma^+$ potential curve. But the $^1\Pi_1$ state has ''mixed'' ($3d\delta_{+2}4p\pi_{-1}+3d\sigma 4p\pi+3d\pi 4p\sigma$) character, may be sufficiently repulsive to cross the higher $^3\Sigma^+$ potential curve on its inner limb near the $v'=5$ level, and thus must be considered a possible perturbing state.

4. $Ca(3d4p\,^3F^0_J)(E=35\,730-35\,897\,cm^{-1})$

Of the possible $^3\Sigma^+$, $^3\Pi$, $^3\Delta$, $^3\Phi$ states, only the $^3\Delta_1$ state could interact appropriately (with the $4s4d\,^3\Sigma^+_1$ components). This state will also be of ''mixed'' ($3d\delta 4p\sigma + 3d\pi_{+1}4p\pi_{+1}$) character, and so must also be under active suspicion as a possible perturbing state, because it may also be quite repulsive in nature.

E. Van der Waals bonding in the $Ca(4s4d\sigma\,^3D_3)\cdot Ar[^3\Sigma^+]$ state

We believe that the Ar atom can penetrate the diffuse $Ca(4d\sigma)$ ''valence'' orbital ($4d_{z^2}$), even along the bond axis where there is a concentration of electron density, because the $Ca(4d)$ orbital is quite diffuse and also has a radial node. As the Ar atom enters the radial node region, the electron–electron repulsion will drop precipitously, resulting in a slight net attraction at $R_o=3.31$ Å. No such attractive $^3\Sigma^+$ state has been observed[17] for the analogous ''valence'' $Mg(3s3d\sigma\,^3D)\cdot Ar[^3\Sigma^+]$ state [where the $Mg(3d)$ orbital is also highly excited and quite diffuse], since there is no ''node'' in the $Mg(3d\sigma)$ orbital, and the interaction is therefore purely repulsive at moderate R. On the other hand, the highly excited Rydberg $Mg(3s4d\sigma\,^3D_3)\cdot Ar[^3\Sigma^+]$ state *has* been characterized,[27] and was shown to be fairly strongly bound, $D_o=800\pm 40\,cm^{-1}$, presumably due to both the *very* diffuse nature of the $Mg(4d)$ Rydberg orbital as well as the presence of the $Mg(4d)$ radial node. The $Mg(3s4d\pi\,^3\Pi)$ and $Mg(3s4d\delta\,^3\Delta)$ Rydberg states[27] have larger D_o values of $1230\pm 50\,cm^{-1}$ and $1200\pm 40\,cm^{-1}$, respectively, as expected, very similar to the D_e value for the $Mg^+(3s)\cdot Ar[^2\Sigma^+]$ ''core'' ion, $1240\pm 40\,cm^{-1}$, since the Ar atom can approach along *angular* nodal axes.

States with potential curve maxima at large R, where v' levels can exist quite happily far above the dissociation limits to the atomic asymptotic products, have been observed directly by others. For example, Tsuchiya *et al.*[3] have characterized the $Hg(6s7s\,^3S_1)\cdot Ne[^3\Sigma^+]$ state, where both the $v'=0,1$ levels are above the $Hg(6s7s\,^3S_1)+Ne$ asymptotic energy, and have shown *experimentally* that there is a maximum in the potential curve of $\sim 150\,cm^{-1}$ at $R=4.0$ Å.

ACKNOWLEDGMENTS

We gratefully acknowledge financial support for this research from the National Science Foundation and the Petroleum Research Fund.

[1] M.-C. Duval, O. Benoist d'Azy, W. H. Breckenridge, C. Jouvet, and B. Soep, J. Chem. Phys. **85**, 6324 (1986).
[2] W. H. Breckenridge, C. Jouvet, and B. Soep, ''Metal-Atom/Rare-Gas Van der Waals Complexes,'' in *Advances in Metal and Semiconductor Clusters*, edited by M. Duncan (JIA, Greenwich, 1995), Vol. 3.
[3] M. Okunishi, K. Yamanouchi, K. Onda, and S. Tsuchiya, J. Chem. Phys. **98**, 2675 (1993).
[4] M. J. McQuaid, J. L. Gole, and M. C. Heaven, J. Chem. Phys. **92**, 2733 (1990).
[5] C. L. Callender, S. A. Mitchell, and P. A. Hackett, J. Chem. Phys. **90**, 2535 (1989).
[6] W. M. Fawzy, R. J. LeRoy, B. Simard, H. Niki, and P. A. Hackett, J. Chem. Phys. **98**, 140 (1993).
[7] C. J. Lee and M. D. Havey, Phys. Rev. A **43**, 6066 (1991).
[8] C. Dedonder-Lardeux, C. Jouvet, M. Richard-Viard, and D. Solgadi, J. Chem. Phys. **92**, 2828 (1990).
[9] M. Czajkowski, R. Bobkowski, and L. Krause, Phys. Rev. A **45**, 6451 (1992).
[10] E. Hwang, Y.-L. Huang, P. Dagidgian, and M. H. Alexander, J. Chem. Phys. **98**, 8484 (1993).
[11] S. Massick and W. H. Breckenridge, J. Chem. Phys. **105**, 6154 (1996).
[12] J. G. Kaup, A. W. K. Leung, and W. H. Breckenridge, J. Chem. Phys. **107**, 10492 (1997).
[13] J. G. Kaup and W. H. Breckenridge, J. Chem. Phys. **107**, 5283 (1997).
[14] J. Jungen and V. Staemmler, J. Phys. B **21**, 463 (1988).
[15] W. Behmenburg, A. Makonnen, A. Kaiser, F. Rebentrost, V. Staemmler, M. Jungen, G. Peach, A. Devdariani, S. Tserkovnyi, A. Zagrebin, and E. Czuchaj, J. Phys. B **29**, 3891 (1996).
[16] S. J. Park, Y. S. Lee, and G.-H. Jeung, Chem. Phys. Lett. **277**, 208 (1997).
[17] Steven Massick and W. H. Breckenridge, J. Chem. Phys. **105**, 9719 (1996).
[18] John G. Kaup and W. H. Breckenridge, J. Chem. Phys. **107**, 6005 (1997).
[19] John G. Kaup and W. H. Breckenridge, J. Chem. Phys. **107**, 6014 (1997).
[20] John G. Kaup and W. H. Breckenridge, J. Chem. Phys. **107**, 5676 (1997).
[21] J. Sugar and C. Corliss, J. Phys. Chem. Ref. Data **8**, 865 (1979).
[22] G. Herzberg, *Spectra of Diatomic Molecules* (Van Nostrand Reinhold, New York, 1950), pp. 318, 319.
[23] *Ibid.*, pp. 221–225.
[24] H. LeFebvre-Brion and R. W. Field, *Perturbations in the Spectra of Diatomic Molecules* (Academic, Orlando, 1986), pp. 100–108.
[25] John G. Kaup and W. H. Breckenridge, J. Chem. Phys. **107**, 4451 (1997).
[26] H. LeFebvre-Brion and R. W. Field, *Perturbations in the Spectra of Diatomic Molecules* (Academic, Orlando, 1986), pp. 101, 106–108.
[27] Steven Massick and W. H. Breckenridge, J. Chem. Phys. **106**, 2171 (1997).